Tele-Impedance based Stiffness and Motion Augmentation for a Knee Exoskeleton Device

Nikos Karavas, Arash Ajoudani, Nikos Tsagarakis, Jody Saglia, Antonio Bicchi and Darwin Caldwell

Abstract— **In this paper, a knee exoskeleton device and its Tele-Impedance based assistive control scheme is presented. The exoskeleton device is an inherently compliant actuated system that was implemented based on the series elastic actuation (SEA) to provide improved and intrinsically soft interaction behaviour. Details of the exoskeleton design are presented. A detailed musculoskeletal model was developed and experimentally identified in order to map electromyographic signals to the antagonistic muscle torques, acting on the human knee joint. The estimated muscle torques are used in order to determine the user's intent and joint stiffness trend. These reference signals are exploited by a novel Tele-Impedance controller which is applied to a knee exoskeleton device to provide assistance and stiffness augmentation to the user's knee joint. Experimental trials of a standing-up motion task were carried out for evaluation of the proposed control strategy. The results indicate that the proposed knee exoskeleton device and control scheme can effectively generate assistive actions that are intrinsically and naturally controlled by the user muscle activity.**

I. INTRODUCTION

The benefits of lower limb exoskeletons in many different applications are already well-known [1], [2]. Assistive exoskeletons can provide motion assistance to elderly people or individuals with impaired legs whose muscles cannot generate the required amount of forces to perform a particular task [3], [4]. Additionally, assistive robotic devices have often been deemed suitable for strength and endurance enhancement of healthy people.

In order for assistive exoskeletons to be widely used and accepted, transparency during operation is a prerequisite. To achieve transparency, the exoskeleton should demonstrate low impedance to the user as well as determine his/her intent and apply forces at appropriate place and time in order to minimize the interaction forces. To satisfy the first requirement we introduce mechanical compliance in the actuation unit of the exoskeleton which decouples the inertia of the motor from the output link to effectively reduce the output mechanical impedance [5]. Additionally, the introduction of elasticity improves the robot's ability to intrinsically absorb impacts and when combined with dedicated control strategies it can be beneficial for the physical human-robot interaction (pHRI) [6].

The ability to deduce the intent of the operator is a fundamental point in designing assistive control schemes for exoskeletons. A common approach is to sense the ground forces of the foot and the joint angles [1] and by using the inverse dynamics model to derive the required joint torques. Another alternative for detecting the user's intent is to utilize electromyographic signals (EMGs) which is a direct measurement from human muscles [4], [7].

Moreover, it is commonly known that the impedance of the human joints varies during motion, a fact which renders the control of exoskeletons highly demanding and the employment of variable impedance systems essential [8].

The contribution of the work is summarized on the development of an intrinsically compliant knee exoskeleton device for inherently soft interaction based on the series elastic actuation (SEA) principle and the implementation of a novel control scheme that permits the natural control of the exoskeleton joint motion using the user muscular activity. Regarding the control scheme, the scope is to incorporate the variability of human joints impedance into the exoskeleton motion regulation using the concept of Tele-Impedance control. Tele-Impedance as an alternative method to unilateral position based control or bilateral force reflecting control was previously proposed during teleoperated tasks which require significant dynamics variation or being performed in uncertain remote environments. The algorithm provides the robot with task-related stiffness profile in addition to position-orientation trajectories [9], [10]. Particularly, we are considering that the stiffness of the exoskeleton joint should be regulated in time according to the flexibility of the corresponding human joint. In other words, the exoskeleton should provide stiffness augmentation for tracking the reference trajectory when the user stiffens his/her muscles and present low levels of compliance when the operator reduces his/her muscle activation. Therefore, the transmission of the forces becomes smoother and the motion assistance more effective while the transparency and comfort of the user is significantly increased.

Several assistive control approaches have been proposed [3], [11], [12], however none of them employ online stiffness regulation based on the user's joint stiffness profile in order to achieve the features mentioned above. A musculoskeletal model of the knee joint, which takes into account the non-linear relationship between muscle activation and joint torques, is developed in order to derive the estimated user torque and the stiffness trend index. The estimated torque

Nikos Karavas, Nikos Tsagarakis, Jody Saglia and Darwin Caldwell are with the Department of Advanced Robotics, Istituto Italiano di Tecnologia, Via Morego, 30, 16163 Genova, Italy {nikolaos.karavas, nikos.tsagarakis, jody.saglia, darwin.caldwell} at iit.it

Arash Ajoudani and Antonio Bicchi are with the Interdepartmental Research Centre "E. Piaggio", Faculty of Engineering, University of Pisa, and with the Dept. of Advanced Robotics, Istituto Italiano di Tecnologia, Via Morego, 30, 16163 Genova, Italy arash.ajoudani at iit.it, bicchi at centropiaggio.unipi.it

is used to determine the user's intended motion and the stiffness trend index (STI) to realise the stiffness of the knee joint which is fed as the stiffness reference to the impedance controller.

The rest of the paper is structured as follows. Section II introduces the exoskeleton hardware. Section III presents the muskuloskeletal model of the knee while section IV discusses the knee model calibration and identification. Section V presents the Tele-Impedance based assistive control scheme while section VI addresses the conclusions.

II. Knee Exoskeleton Hardware

As is illustrated in Fig. 1, the proposed knee exoskeleton consists of two segments (upper and lower) which cover the thigh and shank respectively and the rotational actuation system (CompAct-RS) which drives the joint. The axis of rotation of the exoskeleton joint should be aligned with the axis of rotation of the subject knee joint in order to minimize the mechanical power loss. The exoskeleton interfaces with the wearer by means of four rigid braces and is fastened with four Velcro straps at thigh and shank. In addition, the location of the braces can be adjusted along the structure in order to render the device wearable and functional for different users. Particular attention was paid to fast and easy donning and

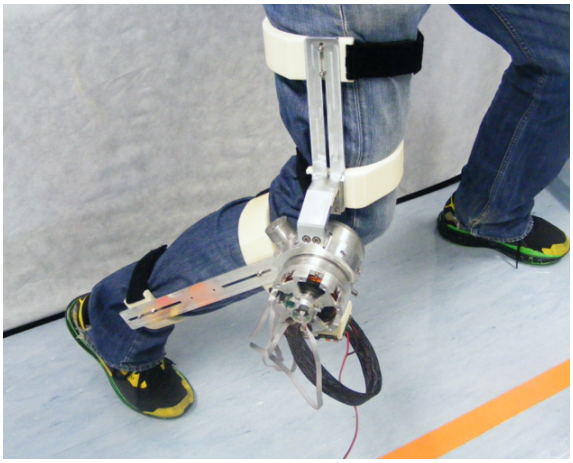

Fig. 1: The Knee Exoskeleton.

doffing (estimated less than one minute). Moreover, the range of motion of the knee exoskeleton in the sagittal plane is between $0^\circ - 120^\circ$ where 0° corresponds to full extension of the knee. Mechanical locks ensure that the actuator operates within this motion range and render the exoskeleton safe to use.

A. Mechatronic System

The knee exoskeleton is energized by a series elastic actuator with offline reconfigurable stiffness. CompAct-RS ([13], [14]) operation is based on the lever arm mechanism with a variable pivot axis (see Fig. 2).

CompAct-RS consists of two main subassemblies. The elastic module that embodies the lever arm mechanism with the reconfigurable pivot point and the motor module. The elasticity is provided by two compression springs which are

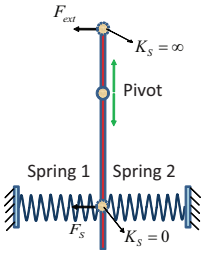

Fig. 2: Functional principle of CompAct-RS; Stiffness can be adjusted theoretically from zero to infinite by varying the position of the pivot.

pre-compressed half of their maximum compression. Note that the location of the pivot point can be adjusted manually by tuning two set screws (see Fig. 3(a)). For this work, the pivot point was set to a position that corresponded to a stiffness value at $K_S = 200$ Nm/rad that was suitable for the execution of the experiments which are described in section IV and V. The elastic module employs one 16 bit

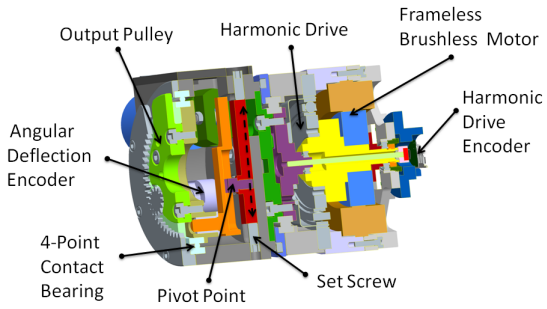

(a)

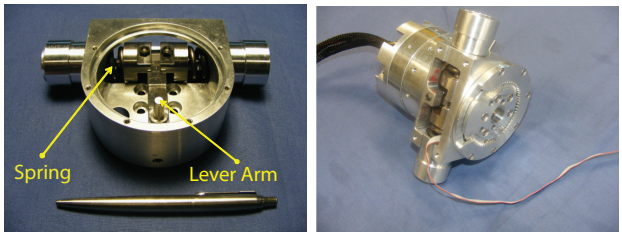

(b) (c)

Fig. 3: a) Section of the CAD assembly of CompAct-RS. b) View of the elastic module. c) Overall view of CompAct-RS.

optical encoder (Avago Technologies) which monitors the angular deflection of the output link and a potentiometer which measures the location of the pivot point. The presence of passive elastic element allows us to avoid the use of an additional torque sensor (which is delicate and expensive), as the elastic torque τ_s is given by the following equation:

$$\tau_s = -K_S(\theta_s)\theta_s. \quad (1)$$

The second subassembly includes a frameless brushless DC motor (Kollmorgen), a harmonic drive CSD 25 with gear ratio 100:1, one optical incremental encoder (MicroE Systems with 12 bit of resolution) for measuring the position of the motor and one 12 bit magnetic absolute encoder

(Austria Microsystems) which monitors the position of the motor after the harmonic drive.

Apparent Stiffness of the Elastic Mechanism: In order to calculate analytically the stiffness of the actuator's output link, we derived its stiffness model from the lever arm mechanism. As it is described in details in [14], for small values of angular deflection the stiffness of the elastic mechanism reads as follow:

$$K_S = \frac{2k_s R^2 l_1^2}{l_2^2} = 2k_s \alpha^2 R^2 \tag{2}$$

where $\alpha = \frac{l_1}{l_2}$ is the ratio of the lever arm, k_s the spring constant and R the distance between the center of rotation of the joint and the point where the force is applied. Note that for acquiring accurate measurements of the torque τ_s we experimentally identified the exact value of the intrinsic stiffness K_S.

B. Mechanical Requirements

For the knee joint one of the most demanding tasks is standing up movement in terms of torque, power and range of motion. Thus, we built a simulation model of human to derive the dynamics of the sit-stand-sit movement cycle [14]. For the simulations we used the anthropometric data obtained from [15] of a male of 82.5 kg with 1.85 m height. Additionally, a subject of 81 kg was instructed to repeatedly stand up and sit down without hand assistance (worst case/highest torques). A Vicon motion capture system with 6 cameras operating at 250 Hz was used to monitor the trackers' position and reconstruct the trajectories of their hip, knee, and ankle joints of both legs. These trajectories were used as input to the simulation model in order to obtain the torque characteristics and correspond to the continuous motion of standing-up, sitting-down and standing up (Fig. 4). The ankle and hip data have not been included due to the page number limitation. From Fig. 4(b) can be resulted

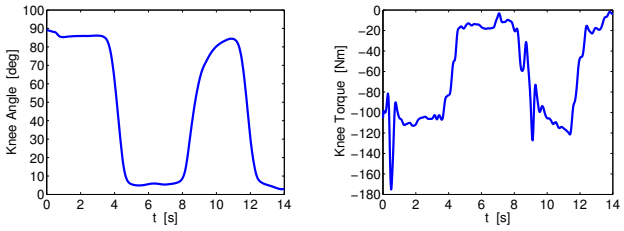

(a) (b)

Fig. 4: Trajectory obtained from Vicon capture system (a) and the corresponding torque (b) of the knee joint.

that the maximum torque, which the knee joint requires, is around 100 Nm (omitting the high peaks). This torque value, which can also be confirmed by biomechanics data in the literature [16], was used as torque specification for the CompAct-RS design. The spikes observed in Fig. 4(b), which were amplified by the numerical differentiation used for obtaining the motion acceleration, are due to the noise of the Vicon system's tracking.

According to the torque specification described above, the maximum achievable angular deflection of the actuator, the amount of stored energy in the springs and the size and weight limitation, we determined the design variables of CompAct-RS [14] shown in Table I.

TABLE I: Specifications of CompAct-RS

Description	Symbol	Value	Unit
Elastic Torque (Max)	τ_s	80	Nm
Torque of motor (Max)	τ_M	1.53	Nm
Elastic Deflection (Max)	θ_s	11	deg
Elastic Energy (Max)	U_s	5.5	J
Allowable Stiffness Range	K_S	$200 \sim 800$	Nm/rad
Diameter	D_A	90	mm
Overall Length	L_A	135	mm
Total Weight	W_A	2.1	kg

III. Musculoskeletal Model of the Knee Joint

In order to account for musculoskeletal bio-feedbacks such as muscular forces-moments, two general approaches have been proposed. Inverse dynamic methods, investigate this problem by means of measurements of the joint positions and applied external forces. However, several drawbacks are attributed to such techniques. For instance, the muscles acting on each joint are grouped and divided to agonist and antagonist blocks and consequently, the external flexion and extension moments are balanced. Therefore, these methods are not reliable enough for individual estimation of muscular forces since a priori assumptions are made on the role of individual muscles during the optimization of a predefined cost function [17]. As a result, alternative solutions which are associated with forward dynamic approaches are proposed. In theses methods, neural commands are extracted and fed to the detailed neuro-musculoskeletal model of the limbs.

By taking into account the precision of the model-based techniques in the estimation of the knee joint stiffness trend and torque by means of antagonistic muscle torques, we exploit and re-identify a detailed musculoskeletal model of the knee joint as follows.

A. Activation Dynamics

Electromyography (EMG) signals inherit patterns of activations of involved muscles. In order to extract muscular activations, the raw EMG signals must be processed. First, these signals are high-pass filtered to remove offsets and movement artifacts. This stage is followed by full rectification techniques. Consequently, the resulting signals are low-pass filtered and normalized in order to provide traces of the neural activation of the muscles. Concerning the motor unit level, it has been observed that muscle force variations with respect to neural commands demonstrate an exponential trend. As a result, activation of the muscles is defined by:

$$a_i(t) = \frac{e^{Au_i(t)} - 1}{e^A - 1} \tag{3}$$

where $a_i(t)$ is the activation of the muscle number i, $u(t)$ corresponds to processed EMGs and $-3 < A < 0$ is a nonlinear shape factor.

B. Contraction Dynamics

Large scale modeling of the muscular force as result of activation dynamics is widely performed based on Hill's muscle model [18] and its extension proposed by Zajac [19]. In such models, the muscle-tendon unit is modeled as a muscle fiber in series with a viscoelastic tendon. Muscle fiber itself is modeled by a contractile element in parallel with an elastic component. The general equation associating the generated force by the contractile element with the muscle-tendon force $F_i^{mt}(t)$ reads as follows:

$$F_i^{mt}(t) = F_i^{max}[f_i(l)f_i(v)a_i(t) + f_{p_i}(l)]cos(\psi_i(t)) \quad (4)$$

where $F_i^{mt}(t) = F_i^t(t)$, with F_i^t, $f_i(l)$, $f_i(v)$ corresponding to the tendon force, normalized force-length and normalized force-velocity curves of the contractile element of muscle number i, and f_{p_i} refers to the passive elastic normalized force-length relation (see details in [19] and [20]). The pennation angle, which is defined as the angle between the tendon and the muscle fibers, is denoted by $\psi_i(t)$ and can be given by the following equation:

$$\psi_i(t) = sin^{-1}(\frac{l_{o_i}^m sin(\psi_{o_i})}{l_i^m(t)}) \quad (5)$$

where $l_i^m(t)$ is the muscle fiber length and ψ_{o_i} the pennation angle at the optimal muscle length $l_{o_i}^m$.

It has been observed that the optimal muscle fiber length varies in response to activation fluctuations [20]. In order to account for such changes, we exploit the following equation:

$$l_{o_i}^m(t) = l_{o_i}'^m(\gamma(1 - a_i(t)) + 1) \quad (6)$$

where $l_{o_i}'^m$ represents the optimal fiber length at maximum activation and γ is the percentage change in optimal fiber length, chosen 15% [20].

C. Musculoskeletal Geometry

The lengths of the muscle-tendon complexes acting on the knee joint are shown to be functions of the knee joint angle [21]. In these works, the muscle length values were fitted to a second order polynomial by means of least squares optimization technique. Consequently, $\bar{l}_i^{mt}(t)$ which accounts for the percentage of segment length (the origin to insertion length relative to its length in full extension of the knee) is defined and identified as follows:

$$\bar{l}_i^{mt}(t) = C_{0_i} + C_{1_i}\theta_{knee}(t) + C_{2_i}\theta_{knee}^2(t) \quad (7)$$

where θ_{knee} represents the knee joint angle in degrees and C_{0_i}, C_{1_i} and C_{2_i} are constants (see [21] for details).

The muscle moment arms $r_i(t)$ of the muscle-tendon unit can be described based on the displacements method proposed in [22] which is defined by:

$$r_i(t) = \frac{\partial l_i^{mt}(t)}{\partial \theta_{knee}}. \quad (8)$$

Consequently, the moment arms are determined as follows:

$$r_i(t) = [C_{1_i} + 2C_{2_i}\theta_{knee}(t)]\frac{180}{\pi}. \quad (9)$$

Once we have estimated the forces (4) and the moment arms (9) of all chosen muscles acting on the joint, we are able to convert the muscle forces to joint torques τ by means of the following equation:

$$\tau(t) = |\sum_{i=1}^{n} \tau_i(t)|_{agonist} - |\sum_{j=1}^{k} \tau_j(t)|_{antagonist} \quad (10)$$

where $\tau_i(t) = F_i(t)r_i(t)$, $\tau_j(t) = F_j(t)r_j(t)$ with n and k being the number of agonist and antagonist muscles acting on the joint, respectively.

D. Stiffness Modeling

It has been shown that a simultaneous increase in antagonistic muscle torques acting on the joint, does not affect the joint torque (as seen in (10)) although does increase joint stiffness [23]. Therefore, we can define the stiffness trend index (STI) as:

$$STI(t) = |\sum_{agonist} \tau_i(t)| + |\sum_{antagonist} \tau_j(t)| \quad (11)$$

and the stiffness of the knee joint as:

$$K(t) = \alpha \times STI(t) + \beta \quad (12)$$

where α (rad^{-1}) and β (Nm/rad) are to be identified constants.

The efficiency of any master-slave teleoperation system is partially governed by proper transmission of the signals (force, position, velocity and etc) between the two. Since the wearable device comes in contact with the human, they together form a local master-slave system. The local Tele-Impedance algorithm (see section V), acting on the exoskeleton, must be in charge of the modeling and tracking of the knee joint stiffness profile. In this outline, the constant values in (12) need to be estimated based on direct measurements of the knee joint stiffness.

An alternative approach is concerned with the stiffness augmentation by means of Tele-Impedance. In such a scenario, one could consider a desired stiffness interval and consequently, the mapping will be defined based on the minimum and maximum values of the STI and the task-oriented stiffness interval. This kind of routine may also be applied for rehabilitation purposes, with osteoporosis patients being one example in which stiffness augmentation is more desirable than stiffness matching. Thus, concerning the above notes, the identification of α and β in (12) will be task-oriented.

IV. Model Identification-Calibration

One healthy subject (male, 27 years old) participated in identification-calibration experiments. Three antagonistic muscle groups (six muscles) which are denoted as being the dominant surface muscles acting on the knee joint were chosen in order to form the musculo-skeletal model of the knee joint. Six electrodes (Bagnoli-16, Delsys Inc.) were attached to the extensor [rectus femoris (RF), vastus medialis (VM) and vastus lateralis (VL)] and flexor [biceps femoris

(BF), semimembranous (SM) and semitendinosus (ST)] muscles. The raw EMG signals were processed (at 1 kHz) and the muscular activities were estimated during the identification experiments as well as during the Tele-Impedance control experiments that are to be described in section V. Model parameters (peak force, optimal fiber length, optimal slack length, pennation angle, nonlinear shape factor and other constants) were extracted from the literature ([17] and [18]-[22]).

For the purpose of minimization of the modeling uncertainty, the parameters of the model must be re-identified based on each user's experimental data. For this reason, we have set up identification-calibration experiments to re-identify the parameters as described below.

A. Model Identification

Considering a reasonable tradeoff between modeling uncertainty and identification complexity, the parameters that were selected to be adjusted based on the identification experiments were: F^{max}, ψ_o, l_o^m, A, C_0, C_1 and C_2.

During the identification experiments, the subject was wearing the knee exoskeleton while having the EMG electrodes attached. In order to take into account the muscle activation of both the knee flexor and the extensor in the model identification, we performed two simple tasks that were involved with each of the antagonistic group of muscles separately. Therefore, during the first task the subject assumed a stand posture (equilibrium position of exoskeleton set to 0°) and was instructed to repeatedly flex and extend his right knee with the minimum possible contraction (flexor contribution) while during the second task the subject was seated (equilibrium position of exoskeleton set to 90°) and was asked to repeatedly extend and flex his knee with minimum contraction as well (extensor contribution). Note that for the calibration experiments we implemented an impedance controller with its stiffness parameter varying from 0 Nm/rad to 200 Nm/rad in intervals of 40 Nm/rad. Additionally, the position of the subject knee joint θ_{knee} was considered to be equal to the position of the exoskeleton joint θ_{exos}. This assumption has been considered for all the experiments of this work. Thus, the torque applied by the human as a result of the changes in the knee angle θ_{exos} during the movement can be given by the following equation:

$$\hat{\tau}_h = \tau_{exos} + \tau_g = \tau_s + (m_{sh} + m_{lseg}) g l_{com} sin(\theta_{exos}) \qquad (13)$$

where τ_{exos} is the torque applied by the exoskeleton and equals to the measured elastic torque τ_s, τ_g the gravitational torque, m_{sh} the mass of shank, m_{lseg} the mass of the lower segment of the exoskeleton and l_{com} the center of mass. Two trials were recorded for each stiffness step. Even trials were chosen for the identification while the odd ones were kept for evaluative analysis of the identification procedure. Movements were carried out at low knee angular velocity and acceleration. For this reason, the inertial moment effects were negligible in our setup.

The data which contains six-channel processed EMGs, torques ($\hat{\tau}_h$, τ_{exos} and τ_g) and knee joint angle changes, were used in order to identify the musculoskeletal model parameters, described in III. Due to the nonlinear dependency between the knee joint torque and the corresponding muscular activities, the nonlinear least square algorithm is utilized for the identification of the model parameters while being constrained to $\pm 10\%$ above/below of their nominal values.

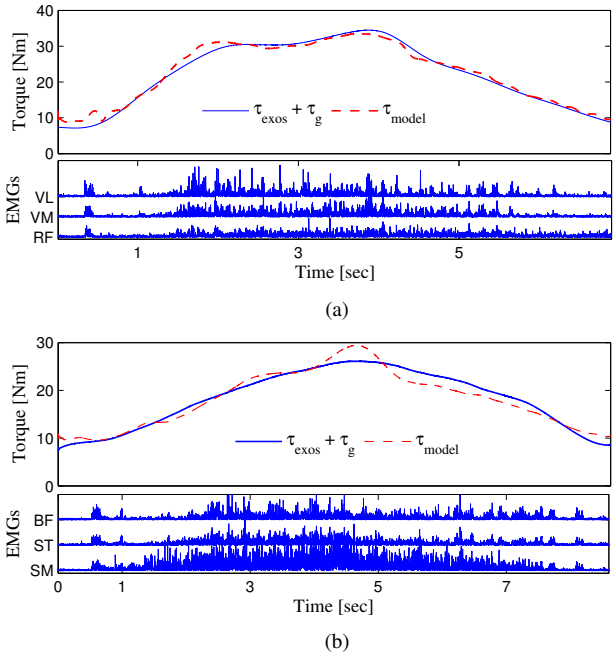

Fig. 5: Comparison of the estimated torque of the knee joint and the one derived from the musculoskeletal model in extension (a) and flexion (b) identification trials.

B. Model Validation

Typical results of the validation of the identified model by means of flexion and extension test trials are demonstrated in Fig. 5(a) and Fig. 5(b), respectively. As is shown in the upper plots, the model provides reasonable tracking of the knee joint torque ($\tau_{exos} + \tau_g$). The corresponding full rectified EMG signals are presented in the lower plots of the figures. The normalised root mean square error (NRMSE) across all test trials (extension and flexion), resulted in an average value of 12.4%.

V. Tele-Impedance based Assistive Control

Impedance control schemes have been already implemented for controlling lower limb exoskeletons. For instance, ANdROS [24] utilizes an impedance controller by applying corrective torques to the wearer's knee based on the deviation from a reference trajectory. In this work the reference trajectory is obtained from a gait pattern which is synchronized by a sensorized unactuated brace worn on the unimpaired leg. On the other hand, the concept of impedance adjustment around joints has been proposed in [12], where the target stiffness, damping and inertia parameters are identified with the Recursive Least Square (RLS) method. Adaptive control schemes have been also used to command powered orthosis

in order to introduce adaptation to the parameters of the human-orthosis dynamic system [8], [11].

A. Interpreting User's Intent and Realizing Knee Joint Stiffness

In the proposed control strategy there is no need to identify the parameters of the human-exoskeleton physical system as the user's intent and his/her stiffness joint trend are obtained from the musculoskeletal model of the knee joint described in III. Fig. 6 depicts the method used for the derivation of

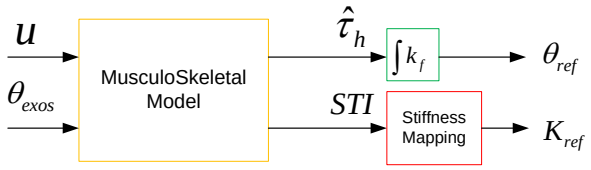

Fig. 6: Schematic of the derivation of the position and the stiffness reference.

the position and stiffness reference for the knee exoskeleton joint. Particularly, to generate assistive torques towards to the direction of motion we select to update the equilibrium position of the knee exoskeleton joint in accordance to the user's intended motion. Thus, the equilibrium position is obtained from the estimated user torque $\hat{\tau}_h$ using the following formula:

$$\theta_{ref} = \begin{cases} \int k_f(\hat{\tau}_h - a)\,\mathrm{d}t & \hat{\tau}_h > a \\ 0 & -a < \hat{\tau}_h < a \\ \int k_f(\hat{\tau}_h + a)\,\mathrm{d}t & \hat{\tau}_h < -a \end{cases} \tag{14}$$

where k_f and a are the sensitivity constant and the noise dead band constant respectively. By deriving the equilibrium position θ_{ref} of the impedance controller from (14), assistive forces augmenting the user desired actions/motions can be generated that are governed by the stiffness parameter of the impedance controller (see Fig. 7).

As it is described in subsection III-D the aim of the exoskeleton device is to provide stiffness augmentation to the user on the basis of his/her stiffness trace. Therefore, we map the STI to the reference stiffness using a desired stiffness range. In this work the desired stiffness range was determined experimentally based on a satisfactory assistance performance related to the task (see subsection V-B). Future work will address the determination of the stiffness range by means of direct measurement/calibration of the human knee joint stiffness.

B. Experimental Evaluation

In order to validate the aforementioned control strategy the sit-to-stand movement was considered. The same subject who participated in the calibration experiments described in section IV was instructed to stand up from a sitting posture while wearing the exoskeleton on his right leg (see Fig. 8) and to support his body weight as possible only on his right leg. The minimum and maximum values of the STI were obtained from the minimum and maximum co-contraction of the thigh muscles of the subject. These were then mapped

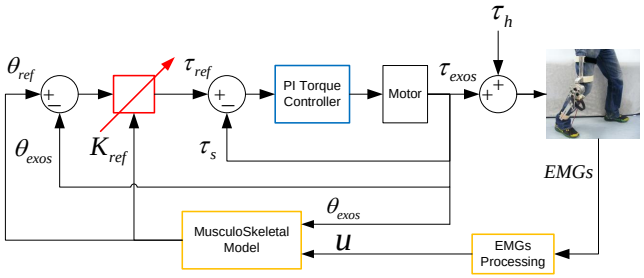

Fig. 7: Block diagram of the implemented Tele-Impedance Controller with stiffness augmentation based on human stiffness trend.

to the desired stiffness range that was set from 0 Nm/rad - 200 Nm/rad. This range was validated through trials in order for the exoskeleton to provide sufficient levels of assistive torques (e.g around 20 Nm).

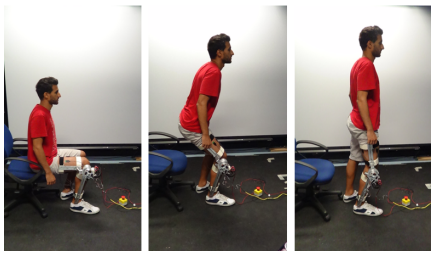

Fig. 8: Standing-up motion task for experimental evaluation.

Fig. 9 illustrates the experimental data during the standing-up motion. The variation of the stiffness reference follows the trace of the subject's joint stiffness. As we expected, the stiffness reference demonstrates a smooth rise in the very beginning of the motion. At a certain point the subject increases his knee joint stiffness to overcome the effect of the increased gravitational torque and to be able to accomplish the motion. Therefore, the stiffness reference increases and the exoskeleton can provide the required amount of assistive torque. In the final phase of the task the subject looses his knee joint (gravitation load reduces in this final stage) in order to decrease the assistive torque provided by the exoskeleton while exploiting the straight knee singular position. In a sense, the subject is intrinsically and naturally controlling the equilibrium position to remain close to the standing posture. Additionally, in Fig. 10 the trend of the knee angle (θ_{knee} equals to θ_{exos}) towards the equilibrium position and the attracting torque which is generated by the exoskeleton are depicted respectively. The noise dead band constant was set at $a = 1$ Nm while the sensitivity constant at $k_f = 0.04$.

VI. Conclusions and Future Work

In this work, a knee exoskeleton was developed which utilises the CompAct-RS, a series elastic actuator, to achieve an improved compliant physical interaction with the operator. The mechatronic system of the CompAct-RS was described and the derivation of the mechanical requirements of its design were discussed. A detailed musculoskeletal model,

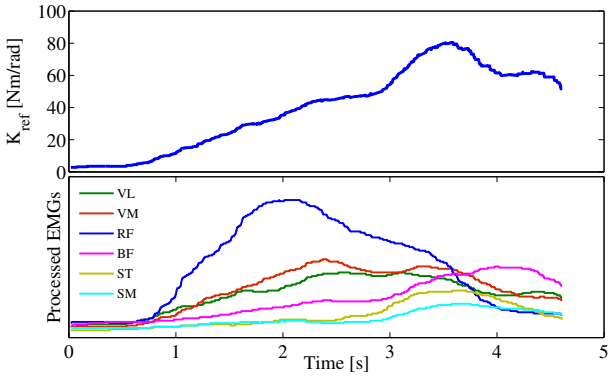

Fig. 9: Reference stiffness during standing up based on the trace of the user's joint stiffness and the processed EMGs of the six muscles.

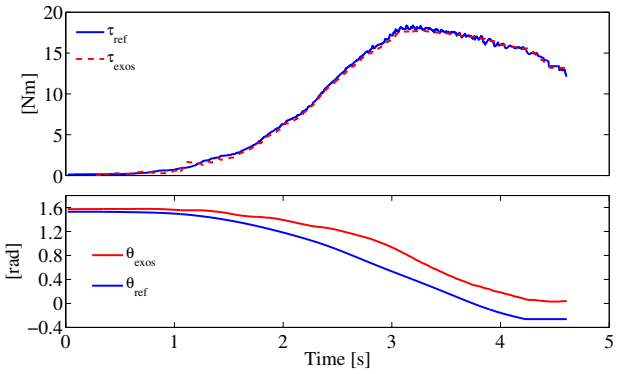

Fig. 10: The torque and position reference and the torque and position of the knee exoskeleton device.

which takes into account the nonlinearity between the muscle activation and the joint torque, was developed in order to obtain the user's intent and his/her stiffness trend through electromyography. These reference signals were fed to an impedance controller which regulates its stiffness parameter based on the user's stiffness trace. Evaluative analysis of the proposed Tele-Impedance based assistive controller was carried out and resulted that the user is able to intrinsically and naturally control the knee exoskeleton device and in addition to receive an effective motion assistance.

The proposed assistive control scheme has the ability to provide stiffness and motion augmentation to the user knee joint. Future work will address the experimentation with different motion tasks such as walking and climbing stairs.

REFERENCES

[1] A. Zoss, H. Kazerooni, and A. Chu, "Biomechanical design of the berkeley lower extremity exoskeleton (bleex)," *Mechatronics, IEEE/ASME Transactions on*, vol. 11, no. 2, pp. 128–138, 2006.

[2] P. Neuhaus, J. Noorden, T. Craig, T. Torres, J. Kirschbaum, and J. Pratt, "Design and evaluation of mina: A robotic orthosis for paraplegics," in *Rehabilitation Robotics (ICORR), 2011 IEEE International Conference on*, 29 2011-july 1 2011, pp. 1 –8.

[3] R. Farris, H. Quintero, and M. Goldfarb, "Preliminary evaluation of a powered lower limb orthosis to aid walking in paraplegic individuals," *Neural Systems and Rehabilitation Engineering, IEEE Transactions on*, vol. 19, no. 6, pp. 652 –659, dec. 2011.

[4] A. Tsukahara, R. Kawanishi, Y. Hasegawa, and Y. Sankai, "Sit-to-stand and stand-to-sit transfer support for complete paraplegic patients with robot suit hal," *Advanced robotics*, vol. 24, no. 11, pp. 1615–1638, 2010.

[5] M. Laffranchi, N. Tsagarakis, and D. Caldwell, "Safe human robot interaction via energy regulation control," in *Intelligent Robots and Systems, 2009. IROS 2009. IEEE/RSJ International Conference on*, oct. 2009, pp. 35 –41.

[6] P. Beyl, M. Van Damme, R. Van Ham, R. Versluys, B. Vanderborght, and D. Lefeber, "An exoskeleton for gait rehabilitation: prototype design and control principle," in *Robotics and Automation, 2008. ICRA 2008. IEEE International Conference on*, 2008, pp. 2037–2042.

[7] C. Fleischer and G. Hommel, "A human–exoskeleton interface utilizing electromyography," *Robotics, IEEE Transactions on*, vol. 24, no. 4, pp. 872 –882, aug. 2008.

[8] J. Blaya and H. Herr, "Adaptive control of a variable-impedance ankle-foot orthosis to assist drop-foot gait," *Neural Systems and Rehabilitation Engineering, IEEE Transactions on*, vol. 12, no. 1, pp. 24 –31, march 2004.

[9] A. Ajoudani, N. G. Tsagarakis, and A. Bicchi, "Tele-impedance: Towards transferring human impedance regulation skills to robots," in *International Conference of Robotics and Automation - ICRA 2012*, Saint Paul, MN, USA, May 14 - 18 2012.

[10] A. Ajoudani, N. Tsagarakis, and A. Bicchi, "Tele-impedance: Teleoperation with impedance regulation using a body-machine interface," *The International Journal of Robotics Research*, vol. 31, no. 13, pp. 1642–1656, 2012.

[11] H. Rifai, S. Mohammed, B. Daachi, and Y. Amirat, "Adaptive control of a human-driven knee joint orthosis," in *Robotics and Automation (ICRA), 2012 IEEE International Conference on*, may 2012, pp. 2486 –2491.

[12] S. Lee and Y. Sankai, "Power assist control for walking aid with hal-3 based on emg and impedance adjustment around knee joint," in *Intelligent Robots and Systems, 2002. IEEE/RSJ International Conference on*, vol. 2, 2002, pp. 1499 – 1504 vol.2.

[13] N. C. Karavas, N. G. Tsagarakis, J. Saglia, and D. G. Galdwell, "A novel actuator with reconfigurable stiffness for a knee exoskeleton: Design and modeling," in *Advances in Reconfigurable Mechanisms and Robots I*, J. S. Dai, M. Zoppi, and X. Kong, Eds. Springer London, 2012, pp. 411–421.

[14] N. C. Karavas, N. G. Tsagarakis, and D. G. Galdwell, "Design, modeling and control of a series elastic actuator for an assistive knee exoskeleton," in *Biomedical Robotics and Biomechatronics. The Fourth IEEE/RAS-EMBS International Conference on*, 2012.

[15] *NASA-STD-3000 Man-Systems Integration Standards*, vol. I.

[16] A. Kralj, R. Jaeger, and M. Munih, "Analysis of standing up and sitting down in humans: definitions and normative data presentation," *Journal of biomechanics*, vol. 23, no. 11, pp. 1123–1138, 1990.

[17] T. Buchanan and D. Shreeve, "An evaluation of optimization techniques for the prediction of muscle activation patterns during isometric tasks," *Journal of biomechanical engineering*, vol. 118, p. 565, 1996.

[18] A. Hill, "The heat of shortening and the dynamic constants of muscle," *Proceedings of the Royal Society of London. Series B, Biological Sciences*, vol. 126, no. 843, pp. 136–195, 1938.

[19] F. Zajac *et al.*, "Muscle and tendon: properties, models, scaling, and application to biomechanics and motor control." *Critical reviews in biomedical engineering*, vol. 17, no. 4, p. 359, 1989.

[20] D. Lloyd and T. Besier, "An emg-driven musculoskeletal model to estimate muscle forces and knee joint moments in vivo," *Journal of biomechanics*, vol. 36, no. 6, pp. 765–776, 2003.

[21] J. Visser, J. Hoogkamer, M. Bobbert, and P. Huijing, "Length and moment arm of human leg muscles as a function of knee and hip-joint angles," *European journal of applied physiology and occupational physiology*, vol. 61, no. 5, pp. 453–460, 1990.

[22] K. An, K. Takahashi, T. Harrigan, and E. Chao, "Determination of muscle orientations and moment arms," *Journal of biomechanical engineering*, vol. 106, p. 280, 1984.

[23] R. Osu, D. Franklin, H. Kato, H. Gomi, K. Domen, T. Yoshioka, and M. Kawato, "Short-and long-term changes in joint co-contraction associated with motor learning as revealed from surface emg," *Journal of neurophysiology*, vol. 88, no. 2, pp. 991–1004, 2002.

[24] O. Unluhisarcikli, M. Pietrusinski, B. Weinberg, P. Bonato, and C. Mavroidis, "Design and control of a robotic lower extremity exoskeleton for gait rehabilitation," in *Intelligent Robots and Systems (IROS), 2011 IEEE/RSJ International Conference on*, sept. 2011, pp. 4893 –4898.